ELSEVIER

Diamond and Related Materials 11 (2002) 1643–1647

DIAMOND AND RELATED MATERIALS

www.elsevier.com/locate/diamond

Effect of film thickness on the stress and adhesion of diamond-like carbon coatings

D. Sheeja*, B.K. Tay, K.W. Leong, C.H. Lee

School of Electrical and Electronic Engineering, Nanyang Technological University, Singapore 639798, Singapore

Received 29 January 2002; received in revised form 29 March 2002; accepted 11 April 2002

Abstract

The important properties of thin films that are used for any applications, especially tribological, are lower internal stress and extremely good adhesive properties. The present investigation examines the effect of film thickness on the compressive stress, adhesive strength (critical load), microstructure and coefficient of friction of diamond-like carbon films prepared under floating conditions (no substrate bias), on silicon substrates. The results show that the compressive stress increases rapidly with thickness in the lower thickness range of up to 50 nm, followed by a slight decrease and thereafter it increases at a slower rate before it delaminates at a thickness of approximately 190 nm. The adhesive strength in terms of critical load shows that the critical load increases with increasing the film thickness up to approximately 110 nm and thereafter it decreases with thickness. The decrease in critical load with thickness, for the films having thickness above 110 nm, is due to the dominant effect of internal stress. The tribological characterisation reveals that the substrate influence on the coefficient of friction is relatively high for the thinnest films ($\sim <40$ nm). The paper also discusses the results of UV and visible Raman spectroscopy as a function of thickness. It is suggested from the characterisation results that appropriate thickness range of the film (prepared under floating condition), is $\sim$40–110 nm.

Keywords: Internal stress; Adhesion; Thickness of the film; Friction

1. Introduction

In the past years, many studies have focused on the synthesis and characterisation of carbon-based coatings such as polycrystalline diamond films and amorphous carbon films [1–7]. The amorphous carbon films are smooth and have many superior properties such as high hardness, high wear resistance, low coefficient of friction, etc., making them suitable for many applications. In addition, the amorphous carbon films can be deposited at room temperature. In recent years, a terminology of diamond-like carbon (DLC) is used to describe the amorphous carbon films. The DLC films can be prepared by different techniques such as radio frequency (RF) plasma enhanced chemical vapour deposition, filtered cathodic vacuum arc (FCVA) technique, etc. The FCVA technique has attracted much attention over the last few years; mainly due to the comparatively good quality film it produces [7].

Generally, compressive stress in the DLC films is significant and is of the order of 1–10 GPa. The high internal stress limits the thickness of the film and it also affects the adhesion of the coating. In the present study, the effect of film thickness on the properties, primarily compressive stress and adhesive strength, of the DLC films prepared by the FCVA technique has been investigated.

2. Experimental details

2.1. Preparation of DLC film

The p^{++} silicon substrates were ultrasonically cleaned with deionized water for 10 min, followed by drying with a static neutralising blow off gun. The samples were then marked on the surface with a marker for the purpose of film thickness measurement and placed in the deposition chamber of the FCVA system. The chamber was then evacuated to a base pressure, lower than 5×10^{-4} Pa. Prior to deposition; argon ions were used to sputter clean the native oxide layer on the

*Corresponding author. Tel.: +65-790-5454; fax: +65-793-3318.
E-mail address: esheeja@ntu.edu.sg (D. Sheeja).

0925-9635/02/$ - see front matter
PII: S0925-9635(02)00109-7

substrate surface. A small area of the sample (marked a couple of lines) was covered with a metal plate during etching for thickness measurement. The arc was ignited by bringing the striker to the cathode surface and the carbon ions were produced from a pure (99.999%) graphite cathode. Off-plane double-bend (OPDB) filter incorporated in the system effectively removed the macro-particles. The substrate holder was in floating bias and the films (approx. 12 samples) were deposited from 20 s to 18 min with the marked line now exposed for the purpose of film thickness measurement. The deposition rate was maintained at approximately 12 nm min^{-1}.

2.2. Characterisation methods

2.2.1. Film thickness and stress

The film thickness and the compressive stress of the films were measured using a surface profiler. Prior to deposition, the samples had been evaluated at three different points on the substrates to obtain the readings of the radius of curvature of the bare substrates (R_o). The samples after deposition were also evaluated at the same reference points to obtain the readings of the radius of curvature of the coated substrates (R). In order to obtain the thickness of the film, the marker lines were erased with alcohol and the surface profiler was used to scan across the boundary of the coated and uncoated surfaces of the unetched portion of the silicon wafer. The stress in the film (σ_s) was then calculated using the following relation (Stoney's equation referred elsewhere [7]).

$$\sigma_s = \frac{E_s}{6(1-\upsilon_s)} \frac{t_s^2}{t_c}\left(\frac{1}{R} - \frac{1}{R_o}\right)$$

where E_s (180 GPa), υ_s (0.26), and t_s are the Young's modulus, Poisson ratio, thickness of the substrate and t_c the thickness of the film.

2.2.2. Adhesive strength of films

A semi-quantitative approach to measure the adhesion of a thin hard coating to its underlying substrate is generally achieved by using a micro scratch tester [8–10]. Here, a diamond indenter is drawn across the coated surface under a progressive load. The load at which the spalling of the coating occurs is defined as the critical load and is proportional to the adhesive strength of the film. The scratch tests were carried out on the samples at different directions to compensate for any effect of substrate orientation.

2.2.3. Microstructure of the films

The microstructure of the films was carried out by using Renishaw Raman-scope systems (UV and visible). The spectra obtained with the ultraviolet (UV) light having a wavelength of 244 nm are more sensitive to the sp^3 content in the DLC film as the excitation energy (5.1 eV) of the UV rays is able to excite the vibrational modes of the sp^3 bonds. Therefore, the amount of sp^3 bonds can be correlated directly instead of inferring from the amount of sp^2 bonds. In order to avoid any structural damage caused by the high photon energy UV laser, the samples were rotated during the measurement. The visible Raman spectra, with lights of 514 nm wavelength (excitation energy of 2.4 eV corresponds to $\pi - \pi^*$ transition at sp^2 sites [11,12]), were obtained for the few thinnest films to study the influence of thickness.

2.2.4. Frictional characteristics of the film

A commercially available pin-on-disk tribometer has been used to study the frictional characterisations of the DLC films. In order to investigate the effect of film thickness on the coefficient of friction, the tests were carried out with a constant load of 1 N, at a constant linear speed of 3 cm s^{-1}, in ambient air (RH, 50%; temperature, 23 °C), with a sapphire counter-face.

3. Experimental results

3.1. Compressive stress in the film

Large compressive stress is known to develop in tetrahedral amorphous carbon films during their growth and is believed to be due to the so-called growth-induced stresses produced by the coating condensation process [13]; and it strongly depends on the deposition process as well as some process parameters. Low compressive stress is one of the primary factors in achieving good adhesion and is crucial in reducing the tendency for stress delamination. The compressive stress of the films, calculated by Stoney's equation, as a function of film thickness is given in Fig. 1. It can be observed from the figure that the stress increases from approximately 2 to 8 GPa as the thickness increases from approximately 3 to 50 nm. Subsequently, it decreases slightly to 7 GPa with increase in the thickness and is maintained until the thickness reaches ~130–150 nm, before the stress reaches to a higher value of approximately 10 GPa at a film thickness of approximately 190 nm. It is also observed that the sample started delaminating at that film thickness.

3.2. Adhesive strength in terms of critical load

The variation of critical load as a function of thickness is given in Fig. 2. It can be seen that there is a trend of increase in critical load from an average value of 1 to 4.5 N, when film thickness increases from 3 to ~110 nm. This is obviously the case, as more load should be needed for the indenter to break through the thicker film into the substrate. These findings are similar to the

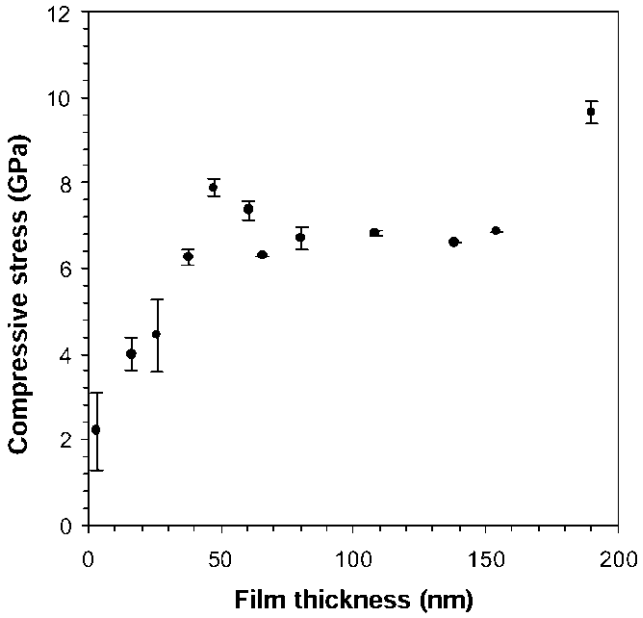

Fig. 1. Variation of compressive stress as a function of film thickness.

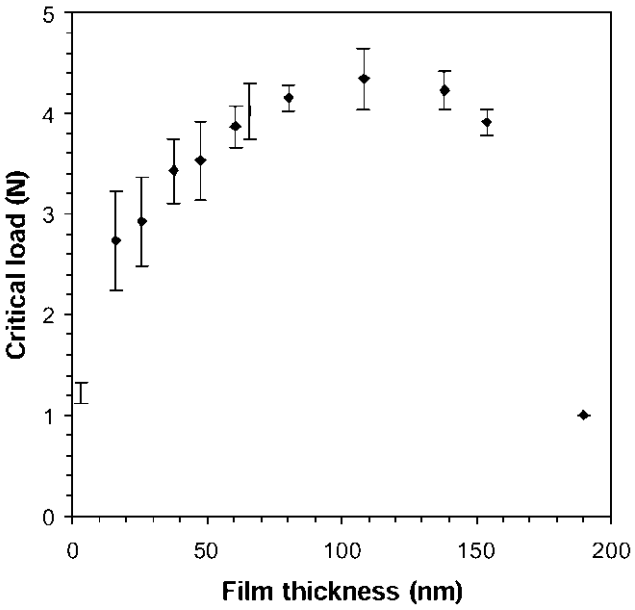

Fig. 2. Variation of critical load as a function of film thickness.

reported results [14], where it states similar trends for coatings on stainless steels, tool steels and cemented carbides. A decreasing trend in the critical load can be observed beyond a thickness of ~110 nm, and is likely be due to the weakening of the coating structure by the high compressive stress.

3.3. Microstructure of the films

3.3.1. Visible Raman studies

Fig. 3 shows the Raman spectra of the films with thickness ranging from ~16 to ~60 nm (no obvious differences in spectra beyond a film thickness of 50 nm). The spectra exhibit a broad Raman intensity distribution in the range of 1400–1700 cm^{-1} centred at 1550 cm^{-1}. However, for thinner films, the absolute intensity of the peak is less obvious. The spectra also show a clear peak at approximately ~965 cm^{-1} regardless of the thickness of the film. This peak corresponds to the second-order phonon scattering from the silicon substrate [15]. The wide peak (1400–1700 cm^{-1}) can be fitted with two peaks; 'G' band at approximately 1560 cm^{-1}, and a 'D' feature at approximately 1360 cm^{-1} and are attributed to sp^2-bonded carbon [16,17]. However, the energy of UV laser at 244 nm (5.1 eV), is sufficient to excite the σ states of both sp^2 and sp^3 sites [17–19]. This allows the Raman spectrum to show a more equally weighted view of vibrational density of states for sp^2 and sp^3 sites. Therefore, quantitative analysis on the structural behaviour of the films was carried out from the UV Raman spectra.

3.3.2. Ultraviolet Raman studies

The UV Raman spectrum is fitted with two peaks, refereed to as 'T' (~1100 cm^{-1}) and 'G' (~1600 cm^{-1}) bands. T-peak position, G-peak position and G-peak width, are deduced from the respective spectra for analysis [17,20]. Fig. 4 shows the variation of T-peak position with thickness, and it can be observed that the T-peak position increases from an almost constant value of 1065 cm^{-1} at film thickness of ~20–45 nm, before reaching a peak of 1100 cm^{-1} at film thickness of ~60 nm. It reduces back to a stable T-peak position of approximately 1070 cm^{-1} from the film thickness of ~80 nm until the film reaches a condition before

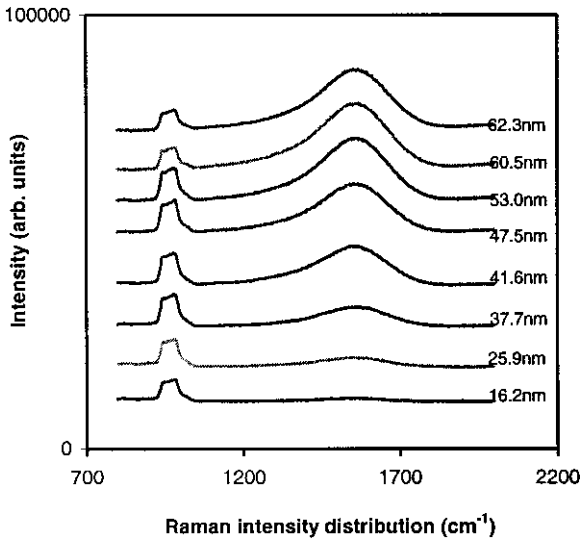

Fig. 3. Visible Raman spectra of films with varied thickness.

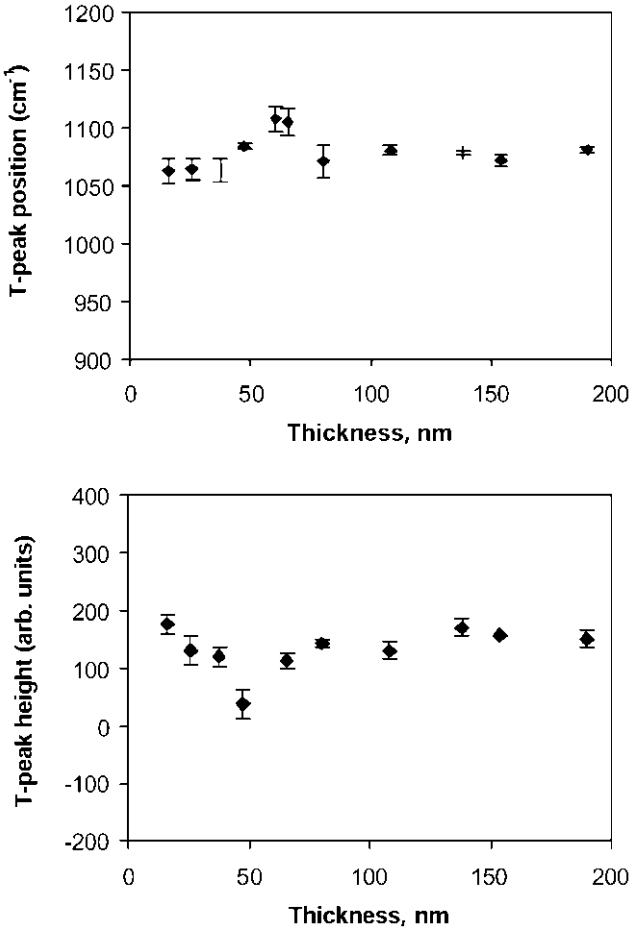

Fig. 4. Variation of T-peak position and T-peak height with film thickness.

delamination. Some studies suggest that the 'T'-peak position is strongly dependent on the sp^3 bonding in the film (T-peak position increases with decrease in sp^3 content) [20]. The intensity of T peak height shown in Fig. 4 decreases as film thickness increases to ~50 nm, then it increases back to a constant value from a film thickness of ~80 nm onwards. Therefore, the trend is providing evidence that the fraction of sp^3 carbon decreased slightly as film thickness increased up to ~50 nm and then increased and resumed the original value after film thickness reaches a value of ~80 nm. It should be noted that the deviation is only slightly larger than the error limit.

3.4. Frictional behaviour of the films

Fig. 5 shows the variation of the coefficient of friction of the films as a function of thickness. It can be observed that the films with thickness less than 40 nm exhibit relatively higher coefficients of friction. The coefficient of friction reaches a steady value of approximately 0.08 for films with thickness larger than approximately 40 nm. The relatively higher coefficient of friction exhibited by the thinner films might be the substrate influence. This interpretation is based on the fact that the Si substrate exhibits a coefficient of friction of approximately 0.5 with sapphire counter-face under the same test conditions.

4. Discussion

It is revealed that the stress increases from approximately 2 GPa at thickness of ~3 nm to approximately 8 GPa at thickness of ~50 nm, before trending slightly downwards to approximately 7 GPa. The downward trend of compressive stress after 50 nm of film growth may be due to the partial relaxation of stress [8,13,21,22]. Partial relaxation of stress occurs when some of the carbon ions fail to penetrate into the growing film due to high stress and forms sp^2 bonded carbon structure on the surface. The slight increment in the process temperature may also prevent the formation of sp^3 bonded carbon structure. The stress maintains at a steady value for thickness ranging from 80 to 150 nm and begins to increase again after that until it reaches a high value of approximately 10 GPa at 190 nm, at which the film starts to delaminate.

The increasing trend of the critical load for film thickness of 3 to 110 nm is likely by the need for increased force to break into the thicker coating of the sample. The decreasing trend of critical load for film thickness of ~110 to ~190 nm, can be explained by the weakening of the coating structure due to the dominant effect of compressive stress.

The results of T-peak position and T-peak height from the UV Raman spectra suggest that sp^3 fraction have remained almost constant until film thickness increases

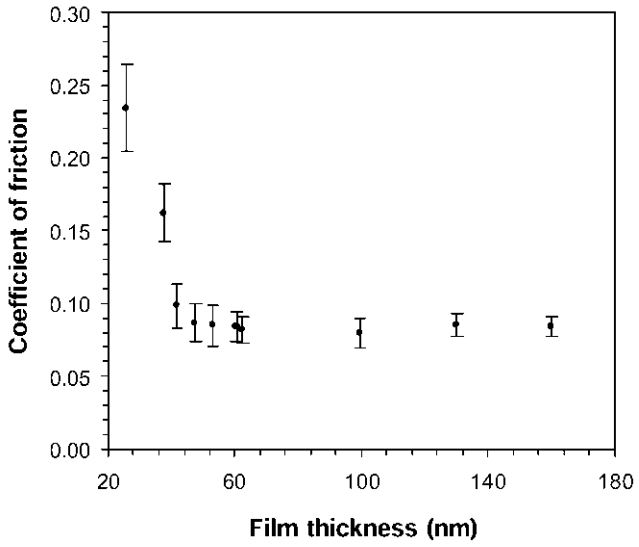

Fig. 5. Variation of coefficient of friction as a function of film thickness (load, 1 N; speed, 3 cm s^{-1} in ambient air).

to ~50 nm, where it decreases slightly to a lower value and recovered back to the normal value at approximately 80 nm, and remained almost constant again until delamination. The likely reason for these observations is the changes in the compressive stress. However, the change of the sp^3 fraction is quite small and can be concluded that the sp^3 content does not vary with much film thickness.

It has been found from the pin-on-disk tribometer study that the coefficient of friction is almost constant regardless of the thickness of the film, except for the thinnest films where the substrate influence on the coefficient of friction is present. However, we have observed from the tribo-test that the sliding life of the thinner films are very short, compared to that of relatively thicker films.

5. Conclusion

Although it has been established that FCVA deposition systems produce relatively good quality coatings, several important factors must be considered before the design stage. It can be suggested from the compressive stress, adhesion and tribological characterisations that, the acceptable film thickness range of DLC prepared under floating conditions is 40–110 nm. The films, which are thinner than 40 nm may be affected by the substrate, and the films that are thicker than 110 nm are weakened by the compressive stress.

References

[1] A. Gangopadhyay, Tribol. Lett. 5 (1998) 25–39.
[2] X.L. Peng, T.W. Clyne, Thin Solid Films 312 (1998) 207–227.
[3] A. Grill, B. Meyerson, V. Patel, J.A. Reimer, M.A. Petrich, J. Appl. Phys. 61 (1997) 2874.
[4] F. Ashrafizadeh, Surf. Coat. Technol. 130 (2000) 186–194.
[5] C. Donnet, Surf. Coat. Technol. 100/101 (1998) 180–186.
[6] P.P. Psyllaki, M. Jeandin, D.I. Pantelis, M. Allouard, Surf. Coat. Technol. 130 (2000) 297–303.
[7] X. Shi, B.K. Tay, H.S. Tan, et al., J. Appl. Phys. 79 (9) (1996) 7234–7239.
[8] A.J. Perry, Thin Solid Films 107 (1983) 167.
[9] P.A. Steinmann, H.E. Hintermann, J. Vac. Sci. Technol. 43 (1985) 2394.
[10] J. Valli, J. Vac. Sci. Technol. A4 (1986) 3007.
[11] J. Wagner, M. Ramseiner, C. Wild, P. Koidl, Phys. Rev., B 30 (1989) 1817.
[12] M.A. Tamor, W.C. Vasssell, J. Appl. Phys. 76 (1994) 3823.
[13] T.H. Roth, K.H. Kloos, E. Broszeit, Thin Solid Films 153 (1987) 123–133.
[14] K. Holmberg, A. Matthews, Coatings Tribology—Properties Techniques and Applications in Surface Engineering, vol. 28, 1994, 282.
[15] T.A. Friedman, K.F. McCarty, J.C. Barbour, M.P. Siegal, D.C. Dibble, Appl. Phys. Lett. 68 (1996) 1643.
[16] J. Schwan, S. Ulrich, V. Batori, H. Ehrhardt, S.R.P. Silva, J. Appl. Phys. 80 (1996) 440.
[17] V.I. Merkulov, J.S. Lannin, C.H. Munro, S.A. Asher, V.S. Veerasamy, W.I. Milne, Phys. Rev. Lett. 78 (1997) 4869.
[18] K.W.R. Gilkes, H.S. Sands, D.N. Batchelder, J. Robertson, W.I. Milne, Appl. Phys. Lett. 70 (1997) 1980.
[19] K.W.R. Gilkes, H.S. Sands, D.N. Batchelder, J. Robertson, W.I. Milne, J. Non-Cryst. Solids 612 (1998) 227–230.
[20] J.R Shi, X. Shi, Z. Sun, E. Liu, B.K. Tay, S.P. Lau, Thin Solid Films 366 (2000) 169–174.
[21] H. Suzuki, H. Matsubara, A. Matsui, K. Shribuki, Jpn. Inst. Metals 49 (1985) 9–15.
[22] D.S. Rickerby, A.M. Jones, B.A. Bellamy, Surf. Coat. Technol. 36 (1988) 661–674.